JOURNAL OF MATERIALS SCIENCE 20 (1985) 2471–2476

Modes of failure under creep/fatigue loading of a nickel-based superalloy

M. R. WINSTONE
Propulsion Department, Royal Aircraft Establishment, Pyestock, Surrey, UK
K. M. NIKBIN, G. A. WEBSTER
Department of Mechanical Engineering, Imperial College, London SW7 2AZ, UK

Crack growth experiments have been carried out under combined creep and fatigue loading at 700° C on a hot isostatically pressed powder nickel alloy. A fractographic investigation has been undertaken of the modes of failure over a frequency range of 0.001 to 10 Hz. The observations indicate that under static loading and at low frequencies failure is intergranular and controlled by creep processes, whereas at high frequencies a transgranular fatigue fracture is obtained. The transition from creep to fatigue behaviour is found to be progressive, and to begin at a lower frequency the higher the ratio of cyclic to mean load. In the transition region a mixed intergranular and transgranular fracture surface is observed, which correlates well with the recorded proportion of creep to fatigue crack growth.

1. Introduction

Many engineering components which operate at elevated temperatures, such as gas turbine discs, blades and guide vanes, are subjected to combined steady and cyclic loading which can give rise to creep and/or fatigue failure. It is the purpose of this investigation to examine the mechanisms controlling failure under this type of loading in a nickel-based superalloy (designated AP1) which is used for gas turbine disc applications.

When load is cycled at elevated temperature, creep-dominated and fatigue-dominated crack growth are both possible depending upon the frequency of loading and the ratio of cyclic to mean load. Previous work [1–5] has indicated that fatigue crack growth is most likely at high frequencies and large load amplitudes, whereas creep-controlled cracking is favoured by high mean loads and low frequencies. When crack growth is cycle-dependent it can usually be described in terms of a stress intensity factor range ΔK [6]; but when creep processes dominate, nonlinear fracture mechanics concepts are required [7–9]. For intermediate loading conditions a creep/fatigue interaction is sometimes observed which may necessitate the application of some form of cumulative damage law.

The aim of this investigation is to establish the modes of failure under creep/fatigue loading as a function of frequency and the ratio of cyclic to mean load in Alloy AP1 at 700° C. It is also intended to relate the appearance of the fracture surface to the proportion of creep to fatigue crack growth that has taken place.

2. Experimental procedure

Alloy AP1 was received in the form of discs 25 mm thick which had been sliced from a hot isostatically pressed billet of 225 mm diameter. The chemical composition and heat treatment of the alloy are presented in Table I. The microstructure had a grain size of approximately 60 μm with about 40 vol% of γ' phase dispersed in a γ-nickel solid-solution matrix.

Standard compact tension test pieces [10], having a width W of 61 mm and thickness B of 25 mm, were cut from the discs and an electro-discharge machined slot of 0.1 mm radius was inserted. Prior to testing at elevated temperature, a fatigue crack of depth a was initiated from the slot at room temperature to a relative crack depth a/W of about 0.25.

The crack growth experiments were carried out

TABLE I Composition and heat treatment of Alloy AP1

Chemical composition (wt% unless otherwise stated)								
Cr	Co	Mo	Ti	Al	Zr	C	B	Ni
14.8	16.9	5.04	3.52	3.98	0.044	0.022	200 ppm	Balance
Heat treatment (AC = air cooled)								
4 h 1100° C, AC,			24 h 650° C, AC,			8 h 760° C, AC.		

at a temperature of 700° C over the frequency range 0.001 to 10 Hz. The wave shape employed was sinusoidal for frequencies of 0.1 Hz and greater, and square-wave for lower frequencies. Two ratios of cyclic to mean load were employed, giving minimum to maximum load ratios R of 0.1 and 0.7. Crack length was measured by a combination of compliance and optical methods to an estimated accuracy of ± 0.1 mm. The fracture surfaces were examined using a scanning electron microscope.

3. Results

3.1. Crack growth tests

The experimental crack-length data were converted to crack growth per cycle (da/dN where N is the number of cycles) using a second-degree polynomial fit through seven points, as recommended in the appropriate standard [10]. The results obtained at the two R ratios and different frequencies are shown in Figs. 1 and 2. It is apparent that the results can be expressed in terms of a stress intensity factor range ΔK by the equation

$$\frac{da}{dN} = C\Delta K^{2.5} \quad (1)$$

where C is a parameter which depends upon R and the frequency f. At the higher frequencies the crack growth is relatively insensitive to frequency, but as the frequency decreases the crack propagation per cycle increases, indicating significant time-dependent effects.

The time-dependent effects can be seen more clearly in Figs. 3 and 4, which show da/dN plotted against frequency at constant ΔK. Above a fre-

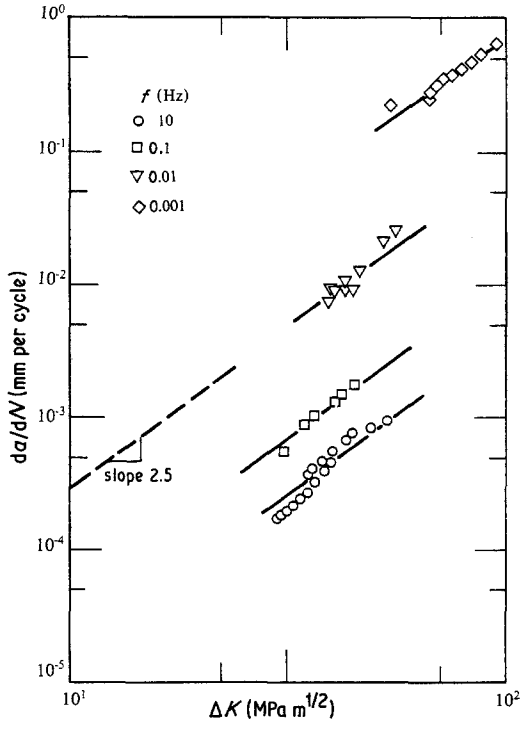

Figure 1 Dependence of crack growth per cycle on ΔK when $R = 0.1$.

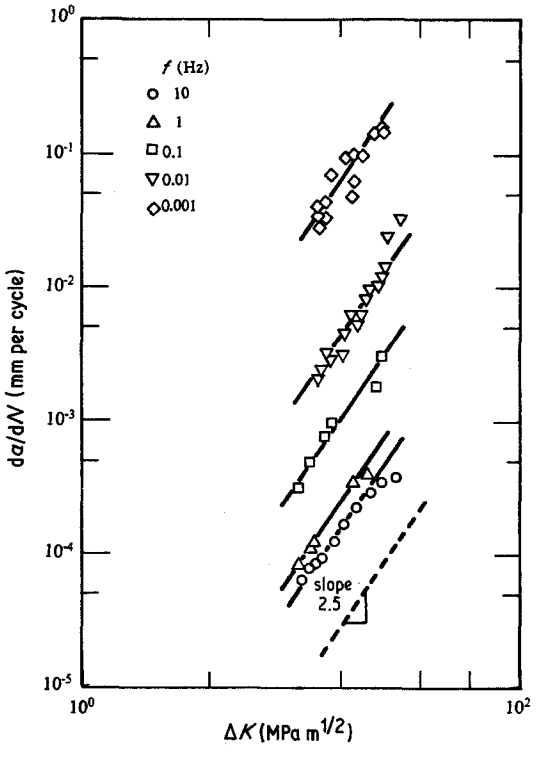

Figure 2 Dependence of crack growth per cycle on ΔK when $R = 0.7$.

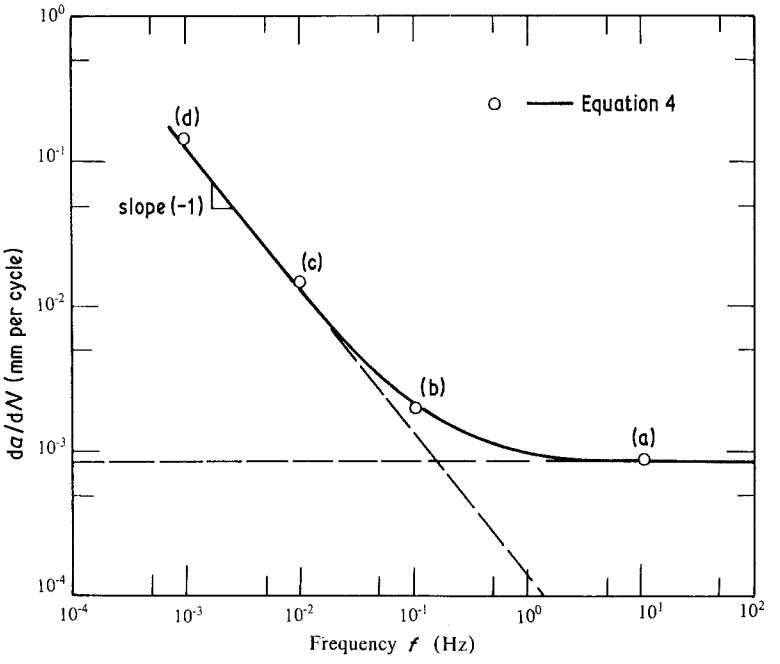

Figure 3 Frequency dependence of crack growth per cycle at $\Delta K = 50\,\text{MPa}\,\text{m}^{1/2}$ when $R = 0.1$.

quency of about 0.1 Hz at $R = 0.1$ (Fig. 3) and above 1.0 Hz at $R = 0.7$ (Fig. 4) relative insensitivity to frequency is obtained. Below these frequencies the graphs indicate an inverse proportionality of da/dN to f.

The frequency dependence can be explained by converting da/dN to crack propagation rate $\dot{a}$ using the expression

$$\frac{da}{dN} = \frac{1}{3600}\left(\frac{\dot{a}}{f}\right) \qquad (2)$$

where da/dN is in millimetres per cycle, f in Hz and $\dot{a}$ in $\text{mm}\,\text{h}^{-1}$. When time-dependent processes control the growth mechanism, $\dot{a}$ will be expected to be constant for given loading conditions and a slope of -1 should be obtained in Figs. 3 and 4. Similarly when cycle-dependent fatigue processes govern, frequency-independence should be observed and a horizontal line obtained in the plots. It is clear that the experimental results demonstrate these features, with a progressive transition between the two modes of cracking.

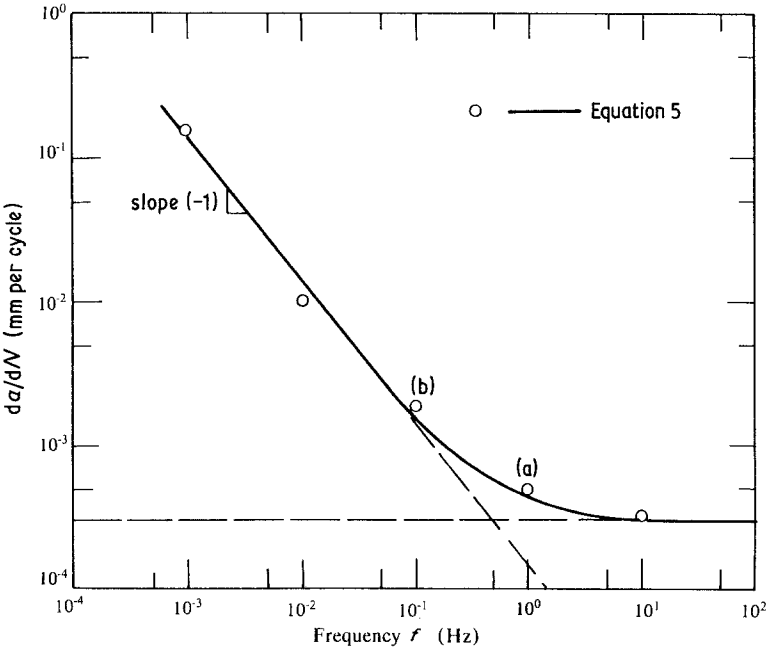

Figure 4 Frequency dependence of crack growth per cycle at $\Delta K = 20\,\text{MPa}\,\text{m}^{1/2}$ when $R = 0.7$.

It has previously been shown for this material [5] that when time-dependent processes dominate, the cyclic crack growth rate can be correlated with data for steady-load creep crack growth, suggesting that creep processes control behaviour in this region. With fatigue mechanisms governing at the higher frequencies, combined creep and fatigue crack growth can be employed to describe crack propagation in the transition range. Assuming linear superposition of the creep and fatigue damage the total crack growth per cycle can be expressed as

$$\frac{da}{dN} = \left(\frac{da}{dN}\right)_C + \left(\frac{da}{dN}\right)_F \quad (3)$$

where the subscripts C and F refer to the creep and fatigue components respectively. The individual components are shown dashed in Figs. 3 and 4. At a stress intensity factor range ΔK of 50 MPa $m^{1/2}$ and $R = 0.1$ (Fig. 3) the creep crack growth rate $\dot{a} = 0.5\,mm\,h^{-1}$ and $(da/dN)_F = 8.0 \times 10^{-4}$ mm per cycle, allowing Equation 3 to be written as

$$\frac{da}{dN} = \frac{0.5}{3600f} + 8.0 \times 10^{-4} \quad (4)$$

For $\Delta K = 20\,MPa\,m^{1/2}$ and $R = 0.7$ (Fig. 4), $\dot{a}$ is again equal to $0.5\,mm\,h^{-1}$ but the fatigue crack growth rate per cycle is 3×10^{-4} mm, giving

$$\frac{da}{dN} = \frac{0.5}{3600f} + 3 \times 10^{-4} \quad (5)$$

Equations 4 and 5 are shown as solids lines in Figs. 3 and 4 respectively. It is evident that they correlate well with the experimental data, and that appreciable creep–fatigue interaction only takes place over about a decade of frequencies at each R ratio. At the low frequencies time-dependent creep crack growth dominates, and at high frequencies cycle-dependent fatigue crack growth does so.

It is apparent from Figs. 3 and 4 and Equations 4 and 5 that a value of $\Delta K = 50\,MPa\,m^{1/2}$ was needed at $R = 0.1$ to obtain the same creep crack growth rate as that measured at $\Delta K = 20\,MPa\,m^{1/2}$ and $R = 0.7$. The larger stress intensity factor range resulted in a fatigue crack growth rate about three times faster at $R = 0.1$ compared with that at $R = 0.7$, causing the transition to fatigue-dominated fracture to occur at a lower frequency at the lower R ratio. However, application of Equation 1 would imply fatigue crack growth approximately a decade faster at the higher ΔK, if C was insensitive to the value of R. It is probable that crack closure effects are significant during fatigue crack growth at the lower R ratio, and hence the high apparent ΔK of 50 MPa $m^{1/2}$ resulted in a smaller fatigue crack growth rate than that predicted by the equation.

3.2. Fractography

The fracture surfaces of the test pieces were examined by scanning electron microscopy to determine the fracture mode. Fig. 5 shows the effect of frequency on the fracture mode with an R ratio of 0.1. At high frequencies (1 to 10 Hz) the fracture was transgranular with some evidence of fatigue striations (Fig. 5a). Secondary cracking along preferred crystallographic planes was common, but intercrystalline cracks were only rarely observed. At a frequency of 0.1 Hz the crystallographic cracking was replaced by secondary grain-boundary cracks, and the fracture surface was a mixture of transcrystalline and intercrystalline features (Fig. 5b). As the frequency was further reduced the extent of intercrystalline cracks proportionately increased. At 0.01 Hz transcrystalline cracking was rare (Fig. 5c) and at lower frequencies the failures were entirely intergranular (Fig. 5d), like those found in steady-load creep tests.

A similar sequence of fracture morphologies was observed when the R ratio was increased to 0.7. At the extreme frequencies of 10 and 0.001 Hz the fracture appearances were the same as those seen at $R = 0.1$ (Figs. 5a and d respectively.) In the intermediate range a greater proportion of intercrystalline fractures was noted at a given frequency for $R = 0.7$ (Fig. 6) than for $R = 0.1$; for example when $R = 0.7$, intergranular features were observed at a frequency of 1.0 Hz (Fig. 6a). Also less transgranular cracking was apparent at 0.1 Hz and $R = 0.7$ (Fig. 6b) than was detected at this frequency when $R = 0.1$ (Fig. 5b).

There was some evidence that the fracture morphology was also a function of the crack growth rate per cycle, with the faster growth rates being associated with a higher proportion of transgranular cracking. However, this effect was small compared with the influence of frequency.

4. Discussion

A correlation can be made between the fracture surface appearances of Figs. 5 and 6 and the crack growth data of Figs. 3 and 4. The points labelled (a), (b), (c) and (d) in these latter figures correspond with the appropriate micrographs of Figs. 5 and 6. It can be seen that the proportions

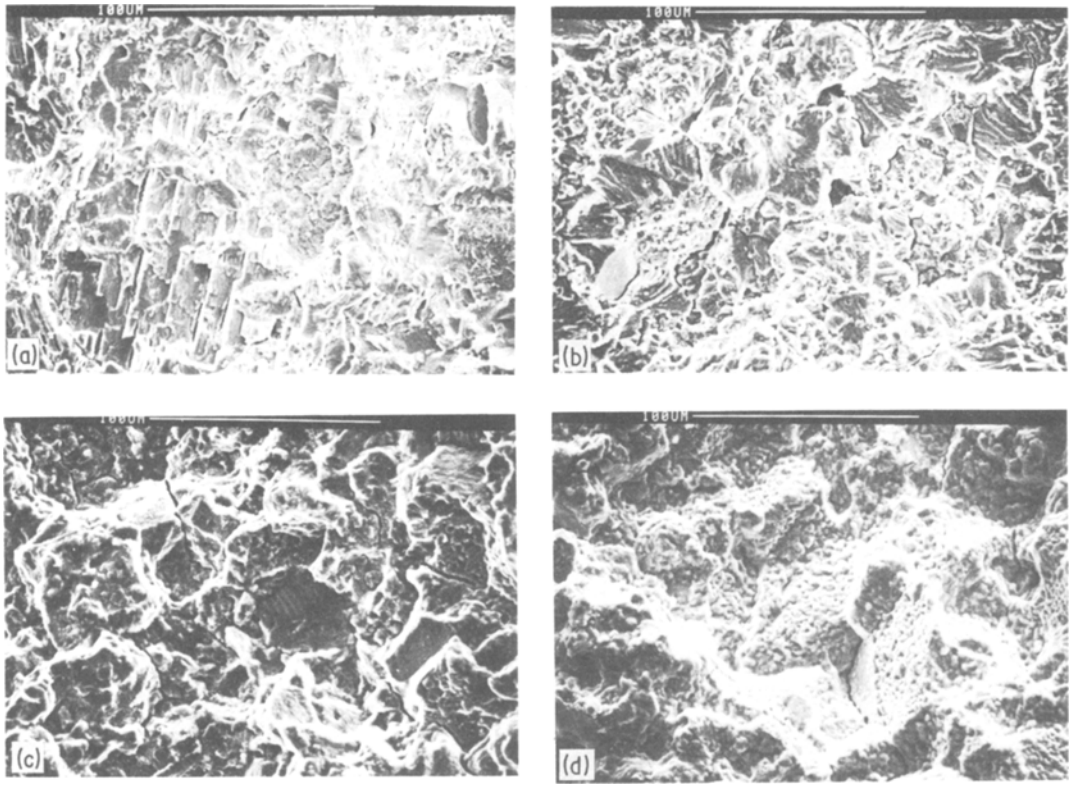

Figure 5 Fracture surfaces when $R = 0.1$: (a) 10 Hz, (b) 0.1 Hz, (c) 0.01 Hz, (d) 0.001 Hz.

of creep to fatigue crack growth correspond with the relative amounts of intergranular and transgranular failure on the fracture surfaces. When fatigue failure dominates as at Points (a) in Figs. 3 and 4, a predominantly transgranular fracture is observed (Figs. 5a and 6a). When both types of crack growth are roughly equal as at Point b in Fig. 3, approximately equal areas of transgranular and intergranular fractures are obtained (Fig. 5b). When creep processes dominate, mainly intergranular fractures are observed (Figs. 5c, d and 6b).

The fractographic evidence therefore provides firm support for the cumulative creep–fatigue model proposed (Equation 3). It is apparent, for the conditions examined, that creep and fatigue damage can be added separately and that each type of crack growth does not significantly influence the other. The maximum cumulative effect is when both contribute equal proportions, resulting in crack growths per cycle of twice the individual values. Interaction is limited to no more than about a decade in frequencies. Reducing the R ratio for a

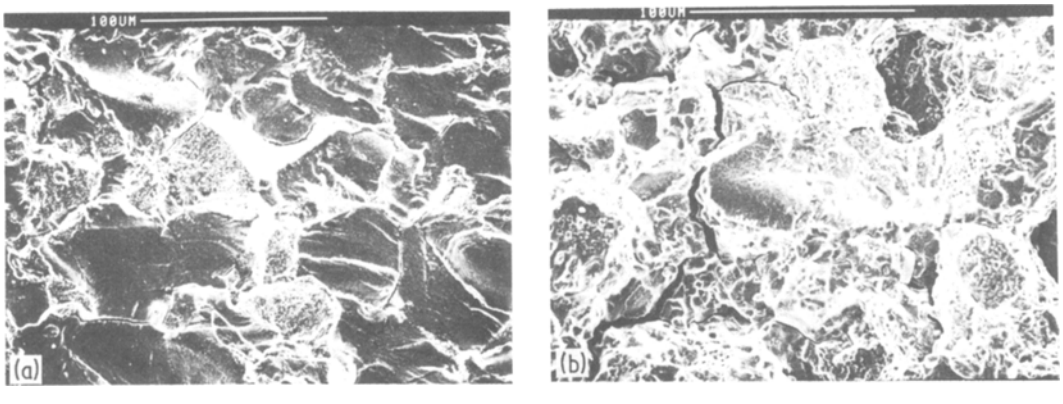

Figure 6 Fracture surfaces when $R = 0.7$: (a) 1 Hz, (b) 0.1 Hz.

given crack growth rate increases the fatigue component, and causes transgranular failure to be extended to lower frequencies.

5. Conclusions

Creep, fatigue, and combined creep and fatigue crack propagation have been observed, and these can be correlated with fracture surface appearances. As the ratio R of minimum to maximum load is reduced, the transition from a transgranular to an intergranular mode of fracture occurs at lower frequencies. Between $R = 0.1$ and 0.7 transgranular fatigue failure dominates at frequencies greater than 1 Hz, and intergranular creep failure at frequencies less than 0.01 Hz. Between these values, mixed-mode fractures are clearly observed which can be related to the measured proportion of creep to fatigue crack growth. It has also been found for the conditions examined that when both processes contribute to the crack propagation mechanism, creep and fatigue damage can be summed linearly to predict the crack growth per cycle.

Acknowledgement

The authors wish to acknowledge financial support provided by the Procurement Executive of the UK Ministry of Defence.

References

1. R. M. PELLOUX and J. S. HUANG, Proceedings of Conference on Creep–Fatigue–Enviroment Interactions, edited by R. Pelloux and M. Stoloff, Wisconsin (TMS-AIME, Warrendale, 1979) p. 151.
2. K. SADANANDA and P. SHAHINIAN, "Cavities and Cracks in Creep and Fatigue", edited by J. H. Gittus (Applied Science, London, 1981) p. 109.
3. D. J. SMITH and G. A. WEBSTER, "Mechanical Behaviour of Materials – IV", Vol. 1, edited by J. Carlson and N. G. Ohlson (Pergamon, London, 1983) p. 315.
4. A. PINEAU, "Fatigue at High Temperature", edited by R. P. Skelton (Applied Science, London, 1983) p. 305.
5. K. M. NIKBIN and G. A. WEBSTER, "Creep and Fracture of Engineering Materials and Structures", Part II, edited by B. Wilshire and D. R. J. Owen (Pineridge Press, Swansea, 1984) p. 1091.
6. P. PARIS and F. ERDOGAN, *J. Basic Eng., Trans. ASME* **85** (1963) 528.
7. M. P. HARPER and E. G. ELLISON, *J. Strain Analysis* **12** (1977) 167.
8. K. M. NIKBIN, D. J. SMITH, and G. A. WEBSTER, Proceedings of Conference on Advances in Life Prediction Methods at Elevated Temperatures, Albany, April 1983) edited by D. A. Woodford and J. R. Whitehead (ASME, New York, 1983) p. 249.
9. G. A. WEBSTER, "Engineering Approaches to High Temperature Design", edited by B. Wilshire and D. R. J. Owen (Pineridge Press, Swansea, 1983) p. 1.
10. ASTM E647-78T, "Tentative Test Methods for Constant Load Amplitude Fatigue Crack Growth Rates above 10^{-8} m/cycle" (American Society for Testing and Materials, Philadelphia 1978) p.662.

Received 27 July
and accepted 10 September 1984